



Transient analysis of a locked rotor/shaft seizure accident involving the EU-DEMO WCLL Breeding Blanket primary cooling circuits

C. Ciurluini^{a,*}, M. D'Onorio^a, F. Giannetti^a, G. Caruso^a, A. Del Nevo^b

^a Department of Astronautical, Electrical and Energy Engineering, Sapienza University of Rome, Corso Vittorio Emanuele II, 244, Roma 00186, Italy

^b ENEA FSN-ING-SIS, ENEA CR Brasimone, Località Brasimone, Camugnano, BO 40032, Italy

ARTICLE INFO

Keywords:

DEMO, Primary heat transfer system
Balance of plant
RELAP5
Accident analysis

ABSTRACT

The EU-DEMO Water-Cooled Lithium-Lead (WCLL) Breeding Blanket (BB) main subsystems to be cooled are the Breeder Zone (BZ) and the First Wall (FW). Each subsystem will be equipped with an independent Primary Heat Transfer System (PHTS). Within the framework of the EUROfusion Work Package Breeding Blanket research program, several accidents belonging to the category of “Decrease in Coolant System Flow Rate” were studied. The activity was aimed at evaluating the blanket and primary cooling systems thermal-hydraulic performances during such transient conditions. A complete model including the BB and related PHTS circuits has been developed at Sapienza University of Rome. A modified version of RELAP5/Mod3.3 system code has been used to perform the calculations. The simulation results showed that a locked rotor/shaft seizure of a BZ or a FW main coolant pump is the most challenging scenario. BZ and FW system behavior has been analyzed following this initiating event with the goal of the design improvement and to individuate the need for preventive measures. The influence of loss of off-site power on the accident evolution has also been investigated. Moreover, management strategies have been proposed for different reactor components. Calculations demonstrate that the current blanket and PHTS design is appropriate to cope with these kinds of accident scenarios.

List of acronyms

BB	breeding blanket
BRC	breeding cell
BZ	breeder zone
COB	central outboard blanket
DIAEE	department of astronautical, electrical and energy engineering
DNBR	departure from nucleate boiling ratio
DWT	double-wall tubes
ESS	energy storage system
EU	EUROFER
EU-DEMO	European Union demonstration fusion power plant
FW	first wall
HEX	heat exchangers
HS	heat structure
IHTS	intermediate heat transfer system
LIB	left inboard blanket
LOB	left outboard blanket
LOSP	loss of off-site power

LR/SS	locked rotor/shaft seizure
MCP	main coolant pumps
OTSG	once-through steam generators
PbLi	lead-lithium
PCS	power conversion system
PHTS	primary heat transfer system
PIE	postulated initiating event
PORV	pilot-operated relief valve
RIB	right inboard blanket
ROB	right outboard blanket
SRV	safety relief valves
TH	thermal-hydraulic
TSV	turbine stop valves
W	tungsten
WCLL	water-cooled lithium-lead

1. Introduction

According to the Roadmap to Fusion Electricity [1], European Union is performing a pre-conceptual design study of a Demonstration fusion

* Corresponding author.

E-mail address: cristiano.ciurluini@uniroma1.it (C. Ciurluini).

power plant (EU-DEMO). The reactor should prove to be capable of producing few hundred MWs of net electricity and of operating with a closed-tritium fuel cycle.

The Breeding Blanket (BB) is one of the key reactor components necessary to accomplish these goals. In fact, it acts as a cooling device, a tritium breeder and a neutron shield [2]. Two breeding blanket concepts are now under investigation in the framework of the EUROfusion research program: the Water-Cooled Lithium-Lead (WCLL) and the helium-cooled pebble bed [3]. WCLL was the option considered for the current simulation activity reported in this work. The reference design [2], relies on water as coolant, liquid lead-lithium (PbLi) as breeder, neutron multiplier and tritium carrier and on EUROFER (EU) as structural material. In addition, a thin tungsten (W) layer is foreseen to cover the plasma facing surface of the First Wall (FW) component. WCLL blanket is composed of elementary units, called BREEDING CELLS (BRC), piled in the vertical (poloidal) direction [2]. Each BRC is divided into two main subsystems: the Breeder Zone (BZ) and the first wall. They are cooled by independent cooling systems, named Primary Heat Transfer Systems (PHTS) [2,4]. The first removes the thermal power generated in the breeder zone by the interactions between the lead-lithium, acting as liquid breeder, and the neutrons emitted by the plasma or due to the interaction with the surrounding materials. The second cools the FW subjected to incident heat flux and the neutron wall load. PHTS circuits are part of the overall Balance of Plant. Different design solutions are under evaluation for this system [5]. The current simulation activity deals with the indirect coupling option that foresees the presence of an Intermediate Heat Transfer System (IHTS) between the FW PHTS and the Power Conversion System (PCS).

One of the major issues regarding the design of BB and related PHTSs is related to the evolution of their performances during abnormal and accidental conditions. In the last years, a large experience was matured in this field. Analyses were performed considering both BB options and using different system codes [6–9]. Within the framework of EUROfusion Work Package Breeding Blanket, a simulation activity was carried out by Department of Astronautical, Electrical and Energy Engineering (DIAEE) of Sapienza University of Rome in collaboration with ENEA research center of Brasimone. The “Decrease in Coolant System Flow Rate” category of accidents was selected to be investigated [10,11]. A complete model of the BB and PHTS circuits was prepared. Transient calculations were performed with RELAP5/Mod3.3 best-estimate system Thermal-Hydraulic (TH) code [12]. A modified version of the code was developed at DIAEE [10,11], where modeling capabilities of fusion reactors were enhanced.

2. Brief description of DEMO WCLL Breeding Blanket and related cooling systems

DEMO reactor normal operations foresee a pulsed operating regime. Two hours of flat-top at full power (pulse) are alternated to ten minutes of dwell time, needed to recharge the central solenoid and to create the vacuum conditions necessary for plasma discharge. The reference parameters and baseline are those of DEMO 2017 concept [2].

2.1. Breeding Blanket

Regarding the blanket component, the design taken into account for calculation purposes is the WCLL BB 2018 V0.6 [2]. It is based on the single module segment approach. The BB component is divided into sixteen identical sectors in the toroidal direction. Each sector is composed of five segments, two Inboard Blankets (Left, LIB, and Right, RIB) and three Outboard Blankets (Left, LOB, Central, COB, and Right, ROB). They are located radially inwards and outwards with respect to the plasma chamber. Segments host the BB elementary cells. BRCs are piled up in the poloidal direction, supported at the back end by water and PbLi manifolds and the EUROFER back supporting structure. The BRC radial-toroidal section is shown in Fig. 1. It refers to COB equatorial cell, the one whose design is at a more mature stage. PHTS circuits inside the BRC consist of FW channels and BZ Double-Wall Tubes (DWT). The former are squared C-shape channels flowing through the overall length of the FW component and equally distributed along with the poloidal height [13]. DWTs are located in horizontal planes at different poloidal elevations and are split into three arrays along the radial direction. Their disposition was optimized during the last years of design activities to match the DEMO requirements related to the BRC [14].

2.2. Balance of plant

PHTS circuits continue outside the vacuum vessel component. In the indirect coupling option [5], BZ PHTS delivers power directly to the PCS by means of two Once-Through Steam Generators (OTSG). The heat removed by the FW PHTS is on the other hand stored in the Energy Storage System (ESS), which is part of the IHTS. The ESS consists of two large molten salt tanks, at different temperatures. HITEC®, a ternary mixture of nitrate salts [15], was selected for nuclear fusion applications [4]. During the pulse, molten salt flows from the cold tank, heats up in the two Heat EXchangers (HEX) thermally coupling the FW PHTS and IHTS and ends up in the hot tank. During dwell, the energy stored is driven to the PCS using four helicoidally coil steam generators. The IHTS and ESS design was developed with the constraint of ensuring a constant turbine load (i.e., constant electricity production and release to the grid)

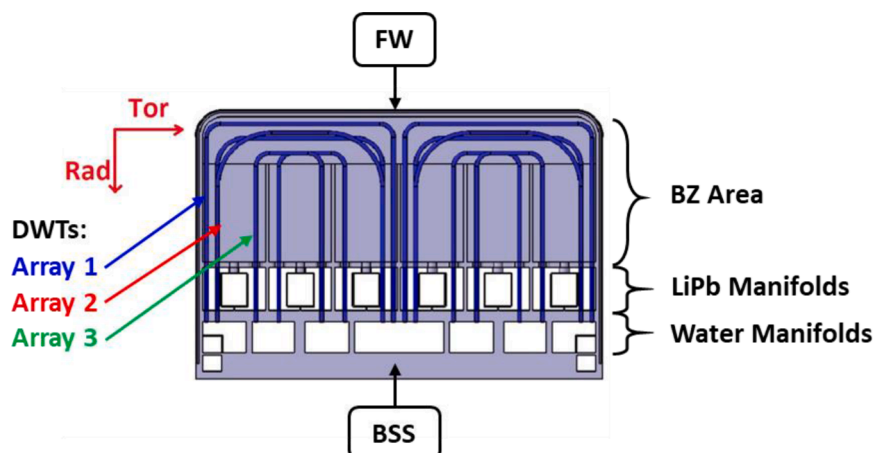


Fig. 1. COB equatorial cell layout, [2].

during both pulse and dwell phases. An overview of BZ and FW PHTSs, as well as IHTS and ESS is shown in Fig. 2. Each PHTS is made up of two loops, symmetrically located around the tokamak circumference. The main system components are: hot and cold rings, sector collectors and distributors, loop piping, heat exchangers/steam generators, Main Coolant Pumps (MCP) and pressure control system (whose principal element is the pressurizer). A more detailed description of the PHTS design is contained in [4,5]. The main TH parameters related to BZ and FW PHTSs, as well as PCS and IHTS, are reported in Table 1.

3. RELAP5 model

3.1. Code and nodalization techniques

To carry out the simulation activity, a full model of the BB component and corresponding PHTS circuits was realized by using RELAP5/Mod3.3 system code [12]. A modified version was developed at DIAEE to better address some issues characteristic of the fusion reactors. New implemented features, involved in the current calculations, regard HITEC® thermal properties [15], and heat transfer correlation (Sieder-Tate [16]). The latter was used to calculate the shell side heat transfer coefficient in the FW HEXs.

General rules to obtain a good mesh were all followed when realizing the reactor model. In particular, the “Slice nodalization technique” was adopted, ensuring the same vertical mesh to system components situated at the same height. Meanwhile, the actual design elevations were strictly maintained for all the vessel equipment and piping. Respecting both these guidelines allows avoiding inconsistencies mainly in the assessment of the natural circulation. In addition, the node-to-node ratio, defined as the ratio between the length of two adjacent control volumes, was always kept below 1.25. In this way, the reactor nodalization is more homogeneous, reducing the possibility of numerical error occurrence. Finally, fluid and material inventories were rigorously maintained for both BB and PHTS cooling systems.

3.2. Blanket models

The blanket system was simulated keeping the toroidal differentiation in sixteen sectors and separating the hydraulic models of BZ and FW primary circuits. Instead, the five segments associated to each sector were collapsed into three pipe components, modeling COB, LOB/ROB and LIB/RIB, respectively. LOB and ROB, as well as LIB and RIB, were

Table 1

DEMO WCLL Breeding Blanket and Balance of Plant nominal parameters.

System	Parameter	Unit	Value
BZ PHTS	Blanket inlet Temperature	°C	295
	Blanket outlet Temperature	°C	328
	Nominal mass flow	kg/s	7662.4
	System pressure	MPa	15.5
FW PHTS	Blanket inlet Temperature	°C	295
	Blanket outlet Temperature	°C	328
	Nominal mass flow	kg/s	2273.6
	System pressure	MPa	15.5
PCS	OTSG feedwater inlet temperature	°C	238
	OTSG feedwater nominal mass flow	kg/s	808
	Steam line pressure	MPa	6.41
IHTS	HEX molten salt inlet temperature	°C	280
	HEX molten salt outlet temperature	°C	320
	HEX molten salt nominal mass flow	kg/s	7048

lumped since they have a similar design (still at a preliminary stage) and the same TH behavior was expected for them. The pipe component related to each segment (or couple of segments) simulates the overall BZ or FW PHTS circuit section inside the vacuum vessel. It is constituted by: inlet feeding pipe, inlet water manifold, DWTs or FW channels, outlet water manifold and outlet feeding pipe. The pipe control volumes are characterized by different hydraulic properties to correctly model each one of the aforementioned components. For the inlet/outlet feeding pipes, geometrical properties and routing were derived from the corresponding CAD model [2], differentiated for each segment. Pipeline features were maintained in the input deck. Regarding the BRC, the most thoroughly analyzed and investigated layout in the last years is the one of the COB equatorial cell (see Fig. 1, [2,13,14]). Design data related to inlet/outlet manifolds, DWTs and FW channels were considered for COB equatorial cell and then scaled for LOB/ROB and LIB/RIB by using material inventories obtained from the CAD model [2]. BZ and FW circuits are thermally coupled within the elementary cell via RELAP5 heat structures. These components are also used for the following functionalities: they account for the BB solid material inventories (EU and W); model the liquid breeder (PbLi); simulate the heat transfer phenomena occurring within the BRC; reproduce the power source terms, i.e., heat flux incident on the plasma facing surface and nuclear heating produced in the blanket materials and fluids; represent the heat losses through pipeline insulation. It is worth noticing that PbLi, even if liquid inside the blanket, was simulated as a solid layer belonging to heat structures components. This approach allows a strong

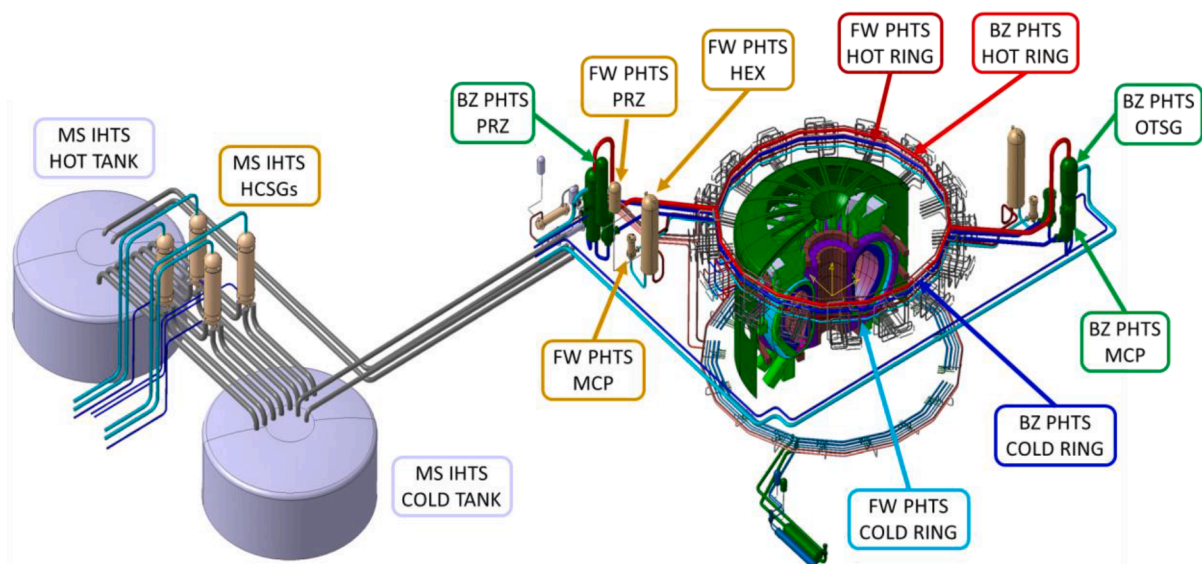


Fig. 2. DEMO reactor overview [4,5].

simplification of the overall reactor model. Although, from the heat transfer point of view, convection in the fluid is neglected and only the conductive term is considered. As widely described in [2,13,14], the breeder velocity while flowing through the BRC is very low, as well as the associated Peclet number. For this reason, the approximation done in the model was considered acceptable for preliminary assessment of the blanket behavior. More details about the BB modeling choices are available in [10,11]. The schematic view of the model related to one blanket sector is shown in Fig. 3.

3.3. PHTS models

Referring to the primary cooling system section outside the vacuum vessel, all main equipment and pipelines were modelled in detail by using one-dimensional components. The schematic view of one (of two) PHTS loop is shown in Fig. 4a and Fig. 4b, respectively for BZ and FW. The CAD model provided the pipeline routing and formulas from [17] were used to calculate the concentrated pressure drops associated with tees, elbows and area changes. A pipe component was adopted to simulate each line separately (hot/cold legs, loop seals, sector collectors/distributors). It is worth mentioning that BZ PHTS has two hot legs and four cold legs (and corresponding pumps), half of the components for each OTSG (Fig. 4a). Instead, in FW PHTS, only two cold legs (i.e., pumps) are foreseen, one per HEX (Fig. 4b). Hot and cold rings have a dedicated model made up of four pipes (one for each quarter) and a multiple junction to manage the connections needed to close the ring and link the component to the loop piping. A further multiple junction (one per circuit) contains the connections between the cold ring and sector distributors and between sector collectors and hot ring. They are equally distributed along the ring circumference, maintaining the tokamak toroidal symmetry. An example of the ring nodalization is shown in Fig. 4c. The PHTS pump system was modelled with RELAP5 pump components provided with a proportional-integral controller to set the rated primary flow. Referring to the OTSG, the same vertical mesh was adopted for the control volumes of all the RELAP5 components simulating the OTSG primary and secondary sides (see Fig. 4a). The primary side inlet and outlet hemispherical heads were modelled with one branch component each. These were connected to a pipe component simulating the tube bundle. The OTSG secondary side was simulated with four pipes, corresponding to lower/upper annular downcomer sections and to lower/upper riser sections. A feedwater line

was added to the input deck by means of a dedicated pipe component. Steam lines were modelled up to the Turbine Stop Valves (TSV in Fig. 4a) and equipped with Safety Relief Valves (SRV in Fig. 4a). PCS SRVs consist of a set of three valves with opening pressures 90%, 95% and 100% of the design pressure, which is 115% of the nominal operating pressure [4,5]. The relief valves related to steps one, two and three were sized to discharge 75%, 37.5% and 37.5% of the nominal OTSG steam mass flow, respectively, considering choked flow occurring in the throat section. Thus, the full SRV set ensures the evacuation of the rated OTSGs steam mass flow with an additional conservative margin of 50%. Turbine bypass valves are not modelled in the input deck. This leads to a conservative prediction of the PCS maximum pressure and, consequently, of the temperature transient in the OTSG primary side. RELAP5 heat structures were used to simulate the thermal transfer taking place inside the steam generator, as well as the component heat losses and the OTSG steel inventory (i.e., thermal inertia). FW HEXs are pure counter-current heat exchangers with PHTS water flowing inside the tube bundle and IHTS molten salt flowing on the shell side. Primary side nodalization is similar to the one of the BZ OTSGs, while secondary side is modelled with an equivalent pipe component (see Fig. 4b). IHTS hot and cold legs were also included in the input deck. Also in this case, heat structures were used to simulate the heat transfer phenomena, the heat losses and the steel inventory related to each heat exchanger. Each PHTS circuit is equipped with a pressure control system (see Fig. 4a,b). Its goal is to keep the water pressure at the required value, compensating the variations induced by eventual coolant temperature fluctuations and, in general, by other transient conditions. The main system component is the steam bubble pressurizer, which is connected to the hot leg of loop one via a surge line. They were both simulated with a dedicated pipe component. The associated heat losses were considered by using heat structures. The pressurizer is provided with On/Off and proportional electric heaters and a spray line connected to the cold leg of loop one and controlled by a valve. These systems are installed to account for under and overpressure transients occurring during both normal operations and abnormal conditions. Pressurizer heaters were simulated with heat structures. The spray valve controller is set to regulate the valve position linearly between a fully closed and a fully open position according to given pressure set points. Pressurizer sprays operate to prevent lifting of the relief valve. The surge and spray line routing was derived from the CAD model [2,4,5], and strictly maintained. If the spray system fails in reducing the pressure, first a Pilot-Operated Relief Valve (PORV), then a

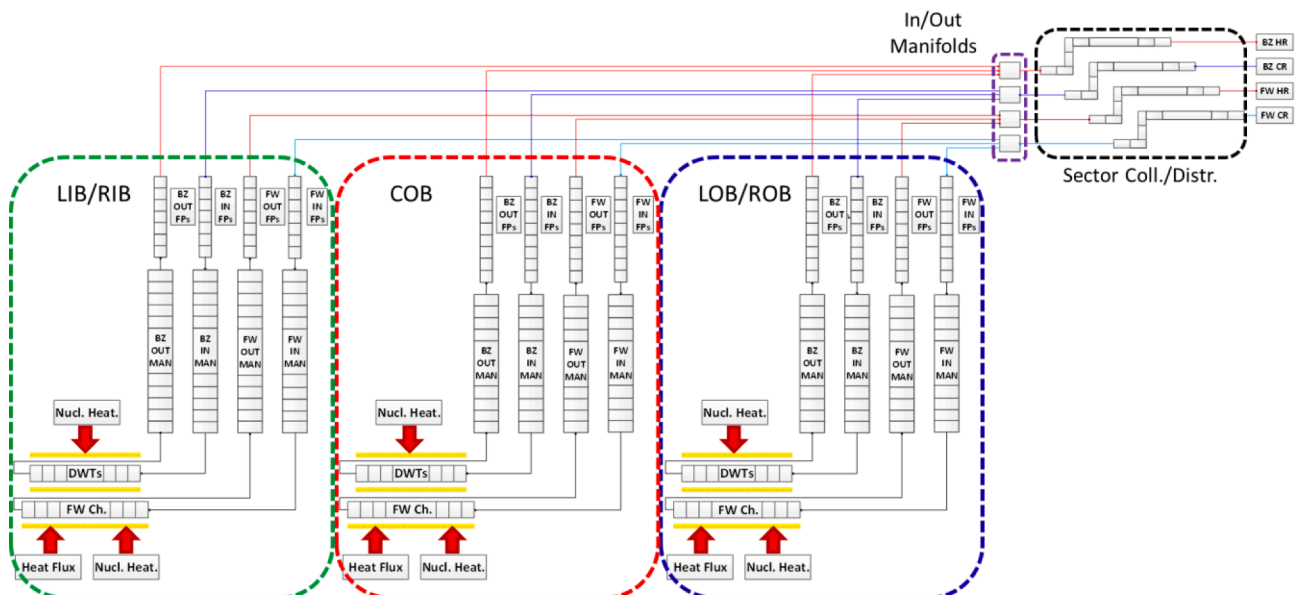


Fig. 3. Schematic view of the TH model related to one blanket sector (of sixteen).

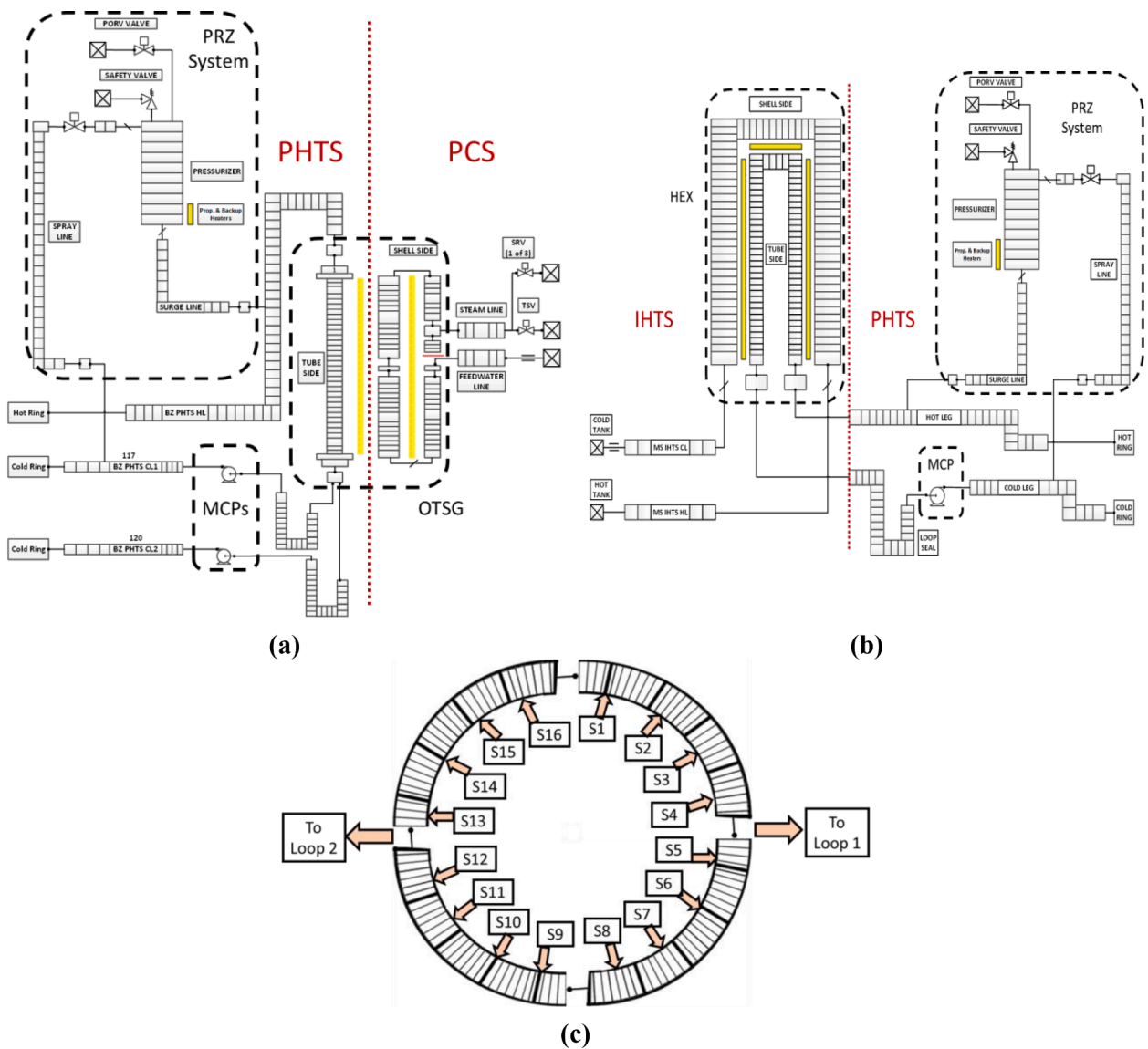


Fig. 4. Schematic view of the TH model related to BZ PHTS loop one (a), FW PHTS loop one (b) and FW hot ring (c).

SRV step into action and let steam from the top of the pressurizer to be discharged to the pressure relief tank. The PORV is more used during normal operations while SRV is more safety oriented. For this reason, the former is provided with a lower setpoint than the latter. PORV and SRV were modelled with RELAP5 valve components. A more comprehensive description of the PHTS nodalization and detailed design data related to the BZ and FW pressure control systems are available in [10,11].

4. Results

Transient analysis involving the BB system and related primary cooling systems has been performed in the last years within the EUROfusion framework of Work Package Breeding Blanket and Balance of Plant research activities. Both operational and accidental scenarios were simulated [10,11]. First, a steady-state calculation of the full plasma power state at beginning of life conditions was performed. Feedwater and molten salt inlet thermodynamic conditions [4,5], were set at the secondary side of BZ OTSGs and FW HEXs, respectively. In addition, a proportional-integral controller was implemented to regulate the heat transfer within the steam generators and heat exchangers by tuning the secondary flow. In this way, the required PHTS water temperature was obtained at OTSG/HEX outlet (i.e., BB inlet), as for DEMO

requirement (295 °C, see Table 1). Finally, the right primary mass flow was achieved in both PHTS circuits thanks to the control system regulating the MCP speed. The results of this steady-state simulation are discussed in detail in [10,11]. This reactor full plasma power state was used as initial condition to perform transient calculations related to “Decrease in Coolant System Flow Rate” accidental category. In this section, part of the outcomes of this simulation activity is presented.

4.1. Selected accidental scenarios and boundary conditions

The selected Postulated Initiating Event (PIE) to be investigated is a Locked Rotor/Shaft Seizure (LR/SS) involving either a BZ or a FW primary pump. The influence on the accidental evolution of the Loss of Off-Site Power (LOSP) is also evaluated (four different cases considered in total).

PIE is simulated by decreasing the rotational velocity of the failed pump from rated value to zero in 1 s. A management strategy for some reactor components is proposed and analyzed. In particular, plasma termination is triggered by one of the following signals: low flow (<80% of nominal value, see Table 1) on primary pumps; high pressure in BZ or FW pressurizer (>16.7 MPa); high temperature in the BZ or FW outlet feeding pipes (2 °C above the saturation temperature at PHTS reference

pressure). Turbine trip is actuated with plasma termination or following the decrease of steam production at OTSG outlet. Both steam flow and temperature are monitored and used as signals. Turbine trip is called if the control system detects a flow below 85% of nominal value (see Table 1) or a temperature below 2 °C above the saturation temperature at PCS reference pressure. The margin adopted for the plasma termination and turbine trip temperature signals is selected considering the typical uncertainty related to a thermocouple reading. Turbine trip activates the PCS feedwater ramp-down and the TSVs closure. As a preliminary tentative, the former is simulated with a linear trend going from the nominal value to zero in 10 s. TSVs are supposed to close in 0.5 s. Regarding the pressure control system, pressurizer heaters are active components that are cut-off if turbine trip is actuated or if a low level is detected in the related tank. Spray flow is interrupted only when all the pumps belonging to a primary system are off, assuming that redundant spray lines are connected to both loops of a PHTS.

Referring to primary pumps, different management strategies are adopted whether LOSP is assumed. Except for the pump affected by the PIE, if power is available, BZ or FW MCPs are stopped when a high-temperature signal (5 °C below the saturation temperature at the PHTS reference pressure) is detected at their inlet. The margin is chosen to avoid cavitation in the component. If off-site power is not present, MCPs trip occurs in correspondence with turbine trip (excluded the failed pump). In this scenario, indeed, the turbine is the only component ensuring the AC power needed for their operation. The proportional-integral controllers (one per primary pump) used in the full plasma power simulation to set the primary flow are disabled. Pump rotational velocity is imposed as a constant boundary condition until the occurrence of MCP trip. After that, the component coast-down is ruled by the torque-inertia equation. Also, IHTS mass flow is managed differently according to the presence or not of off-site power. If available, HITEC® flow is ramped down 10 s after the PIE, assuming a preliminary linear trend lasting 10 s. Conservatively, it is assumed that PIE occurs at the end of plasma pulse when the ESS cold tank is nearly empty. If LOSP is assumed, IHTS flow is ramped down following the turbine trip. Even in this case, the steam turbine is the only element ensuring the AC power needed for the molten salt pumps operation. The proportional-integral controllers adopted in the full plasma power scenario to set the right temperature at BB inlet and acting on PCS feedwater and IHTS flow are disabled. At their place, boundary conditions are imposed at OTSGs/HEXs secondary side inlet by using time-dependent junctions responding to the actuation logics described above.

The plasma ramp-down curve is derived from [18] and reported in [11] as a relative trend to be applied to both nuclear heating and incident heat flux. After plasma shutdown, only decay heat is left (nearly 2% of the reactor rated power). Simulations are run assuming PIE occurring after 100 s of full plasma power state. Such initial phase is represented in the figures of the following sections with a gray background. The timeline is reset in the plots to have PIE at 0 s. Transient calculations last 9000 s (2.5 hr), for an overall simulation time of 9100 s. Different time steps are used. Initially, when the transient dynamic is expected to be faster, a lower time step is used (5.0×10^{-3} s). In the final part, this parameter is increased (1.0×10^{-2} s) to speed up the simulations.

For each transient calculation analyzed in this paper, there is an analogous one in [11] related to partial loss of flow accident. The only difference between these two scenarios is that LR/SS causes failed pump velocity to drop to zero nearly instantaneously, while, in the partial loss of flow accident, failed pump decelerates following the torque/inertia equation. Hence, in the first case, the loss of primary flow is quite faster and the resulting temperature transient for both blanket component and PHTS circuits is more severe. For this reason, analysis of the results in the following sections is focused on the early time (200 s) after the PIE occurrence. In the long term, both initiating events have similar accidental evolution and BB PHTS behavior. The related discussion is available in [11].

4.2. LR/SS involving FW PHTS primary pump without LOSP

The PIE involves FW PHTS loop 1 primary pump. No loss of off-site power is assumed. As previously stated, failed pump rotational velocity drops to zero in one second. The control system immediately (<0.5 s) detects the flow decrease (see Fig. 5a) and actuates the plasma shut-down. As a consequence, also turbine trip is triggered, followed by PCS feedwater coast-down and TSV closure.

Since off-site power is available, loop 2 pump continues to operate at nearly nominal conditions (see Fig. 5a). Its primary flow is unevenly distributed between the sixteen sectors, according to their position. The highest flow rate is experienced in sector 13 since it is the nearest to loop 2 (i.e. the operative pump, see Fig. 4c). On the contrary, sector 4, the nearest to the failed pump, is the one experiencing the minimum cooling flow and the most severe temperature transient. Mass flow trends plotted in Fig. 5b for sectors 4 and 13 envelop the ones related to all the other sectors (not reported). The same rationale is used for the FW PHTS water temperatures at blanket inlet and outlet. Only the temperatures of sector 4 (worst case) and sector 13 (best case) are plotted in Fig. 5c. The maximum water temperature registered at blanket outlet is 347 °C and it occurs 20 s after the PIE occurrence. In a short time interval (few seconds) around this event, the steam quality in the final section of FW channels reaches nearly 10% (Fig. 5d). However, the associated Departure from Nucleate Boiling Ratio (DNBR) calculated by the code is $\gg 1$. No thermal crisis is thus expected in the cooling channels. Nevertheless, it must be noted that the blanket model prepared for the current simulation activity is not able to investigate the local behavior of FW component since no poloidal differentiation is performed. In addition, the heat flux used as boundary condition is the average one related to the overall reactor. Although, this parameter varies significantly along the tokamak poloidal dimension, arriving at values far higher than the mean. In conclusion, the DNBR computed by the code is only an average parameter evaluated for the overall FW component. For this reason, more detailed analyses are needed in the future to evaluate the DNBR at different poloidal locations inside the BB.

Material temperatures in the FW component are reported in Fig. 5e, for both tungsten and EUROFER. Sector 4 is chosen as worst case and COB is used as reference segment. The effect of the water temperature spike is not visible in the figure, and this is due to the FW thermal inertia that, even if low, is enough to absorb the thermal fluctuation. What is experienced by FW materials is the temperature decrease caused by the plasma termination. Water temperature increase also produces a pressure peak in the FW system (Fig. 5f). Although, the pressure transient is quite mild, and it is managed by the pressurizer spray system, avoiding PORV intervention. FW sprays are still operative since loop 2 pump is on and provides forced circulation.

One last phenomenon to be discussed is the flow inversion in loop 1, highlighted by the negative values shown in Fig. 5a. It is produced by the significant pressure drops associated to the blanket component [10,11]. For this, part of the flow provided by loop 2 pump goes through loop 1 in the reverse direction instead of flowing in the BB sectors. The reverse flow causes a temperature inversion in the corresponding loop.

Regarding the BZ PHTS, since LOSP is not assumed, all the primary circuit pumps keep on running at nominal velocity, ensuring nearly the rated primary flow. After plasma termination, the water temperatures at blanket inlet/outlet converge to almost a common value since only decay heat is left. As an example, Fig. 5g shows the temperatures related to sector 1. The pressure spikes reported in Fig. 5f,h for the PHTS and PCS are due to the management strategy adopted for the secondary system. In fact, plasma termination and turbine trip occur simultaneously. Plasma power decreases with an exponential trend lasting nearly 40 s (before dropping to decay heat). Instead, feedwater is linearly reduced to zero in 10 s and, above all, TSVs close in 0.5 s. This misalignment between the power source and the heat sink cooling capability causes a power surplus that is dissipated by the corresponding PHTS and PCS pressure control systems. In particular, all three steps of

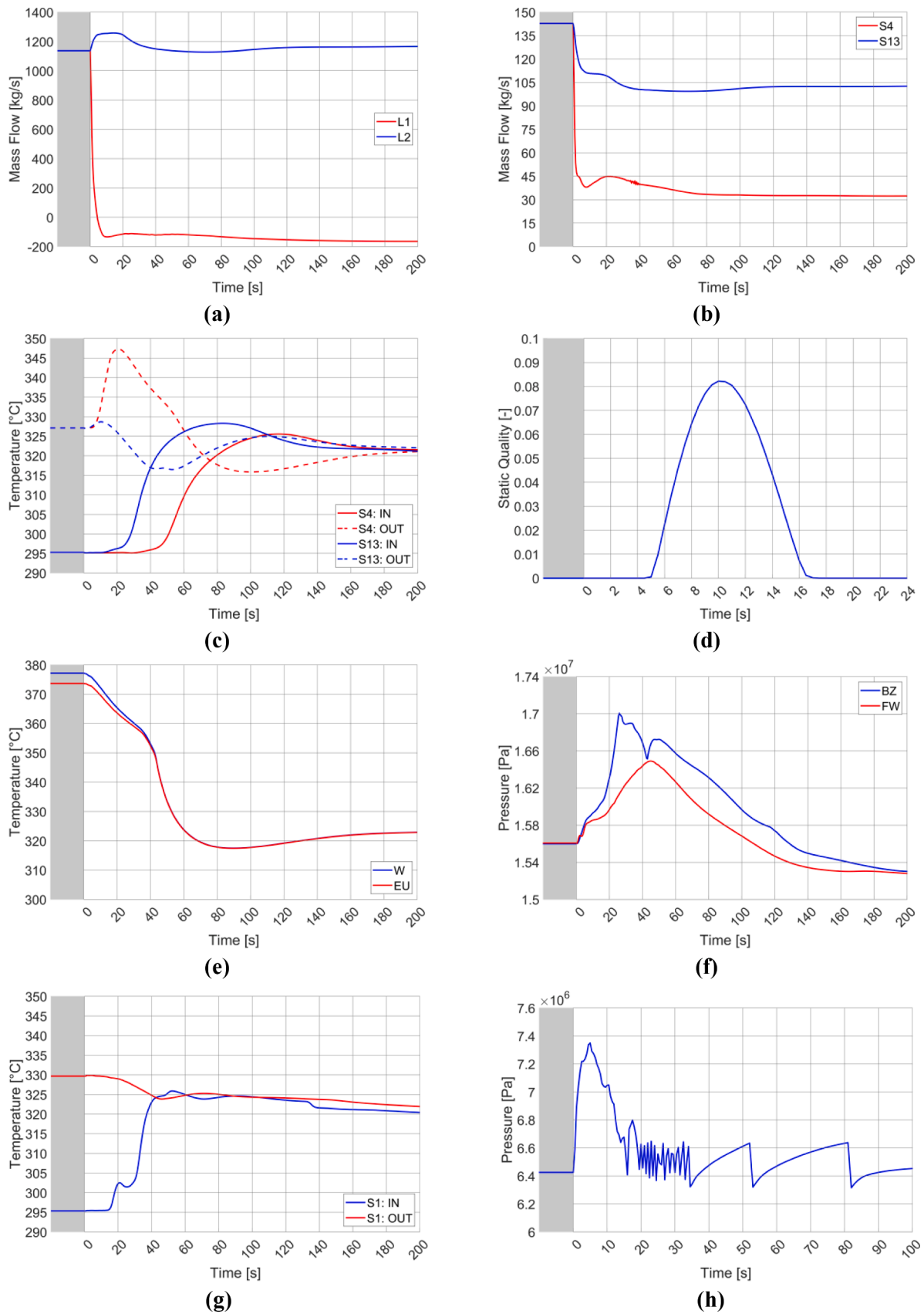


Fig. 5. LR/SS involving FW PHTS loop 1 pump without LOSP: FW primary pumps mass flow (a); FW sectors mass flow, sector 4 and 13 (b); FW PHTS water temperatures at BB inlet/outlet, sector 4 and 13 (c); Steam quality at FW channels exit, sector 4 (d); Tungsten (W) and EUROFER (EU) temperatures related to FW component in sector 4 COB segment (e); FW and BZ PHTS pressures (f); BZ PHTS water temperatures at BB inlet/outlet, sector 1 (g); PCS pressure (h).

SRVs intervene at the secondary side, while BZ pressurizer sprays and PORV manage the pressure transient in the primary circuit. In both systems, pressure does not exceed the design value, demonstrating the appropriateness of the PHTS and PCS pressure control function.

4.3. LR/SS involving BZ PHTS primary pump without LOSP

LR/SS accident affects one of the pumps of BZ PHTS loop 1. As for the previous scenario, the component low flow is immediately (<0.5 s) detected by the control system, triggering plasma termination and turbine trip.

As shown in Fig. 6a, the BZ pumps not affected by the PIE are still working thanks to the availability of off-site power. While loop 2 pumps keep operating at nearly nominal conditions, the active component of loop 1 increases the provided mass flow. From its point of view, two alternative flow paths are now available: the blanket sectors and the

loop 1 branch where the failed component is situated. The pressure drops associated with the second path are significantly lower, even with the broken pump acting as a minor head loss. For this reason, the curve of hydraulic resistance associated with loop 1 active pump decreases, while the rotational velocity is maintained constant being imposed as a boundary condition (see Section 4.1). Consequently, the pump surges the provided mass flow and decreases the head. The reverse flow in the branch hosting the failed component (negative values of the red line in Fig. 6a) does not cause temperature inversion in the corresponding loop. Looking at Fig. 4a, it is possible to note that each BZ OTSG is connected to the cold ring by means of two pipelines, each one equipped with a primary pump. If one of them crashes, as in this transient, the other ensures the flow through the loop in the right direction. Referring to FW system, only one primary pump is present in each loop, hence, both flow and temperature inversions occur, in case of component failure.

The total BZ flow is distributed among the sixteen sectors according

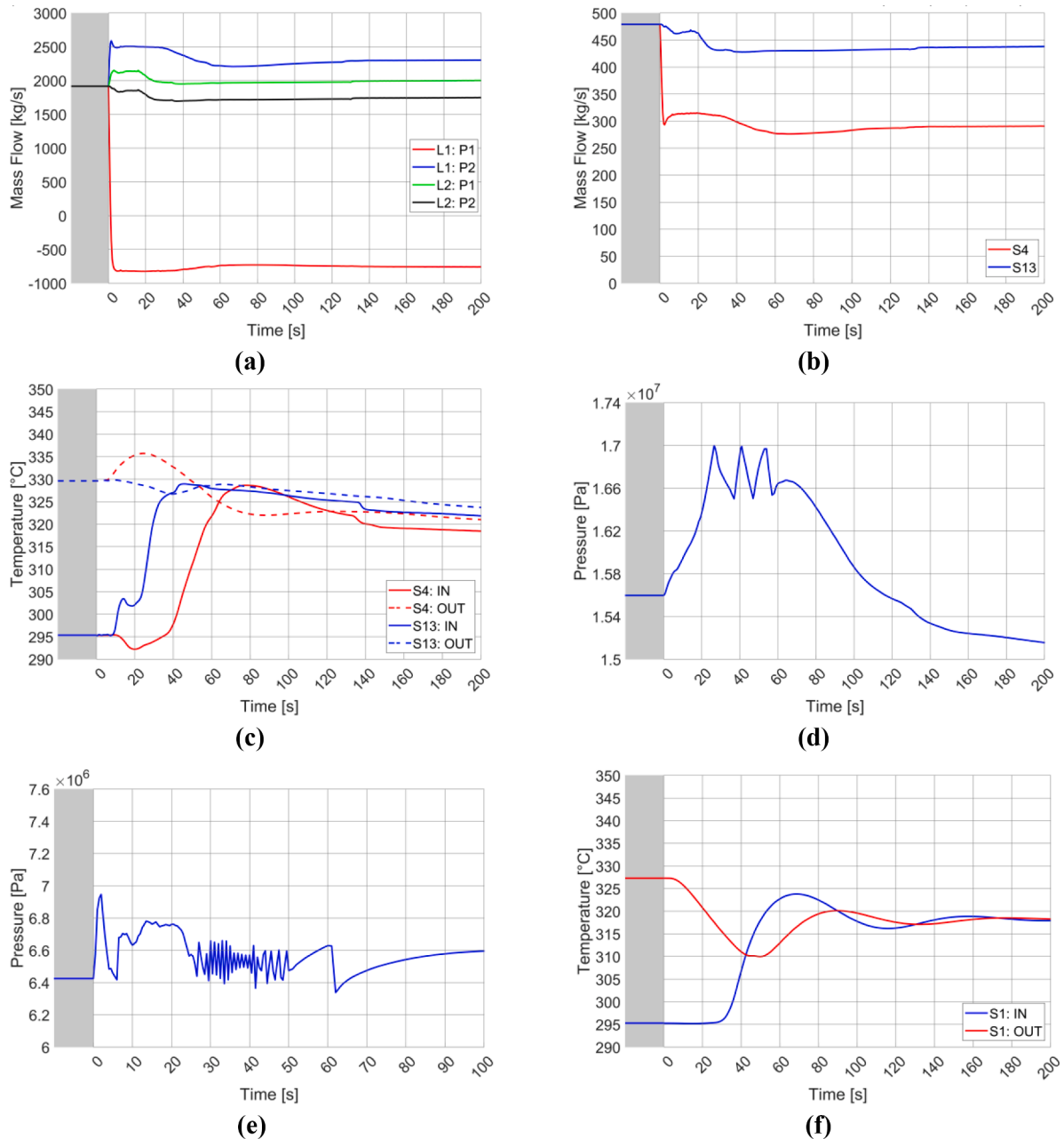


Fig. 6. LR/SS involving BZ PHTS loop 1 pump without LOSP: BZ primary pumps mass flow (a); BZ sectors mass flow, sector 4 and 13 (b); BZ PHTS water temperatures at BB inlet/outlet, sector 4 and 13 (c); BZ PHTS pressure (d); PCS pressure (e); FW PHTS water temperatures at BB inlet/outlet, sector 1 (f).

to their relative position with respect to the failed pump. For this reason, even in this case, sector 4 represents the worst case and sector 13 the best one, enveloping all the others. Mass flows and water temperatures at BB inlet and outlet are plotted for the sectors of interest in Fig. 6b and Fig. 6c, respectively. The maximum water temperature detected at BB outlet is 335.5 °C (at 25 s after the PIE occurrence). It is well below the saturation temperature at the nominal system pressure (15.5 MPa), thus no thermal crisis is expected within DWTs. The lower peak with respect to FW system is due to the large thermal inertia offered by PbLi flowing in the BZ area.

The phenomenology behind the occurrence of the pressure spikes shown in Fig. 6d and Fig. 6e, respectively referred to PHTS and PCS, has already been discussed in the previous section. Another aspect is worth to be pointed out. In this case, the pressure peak experienced in PCS system (Fig. 6e) is reduced with respect to the analogous in Fig. 5h. At the same time, more PHTS PORV interventions (represented by the

number of teeth in the sawtooth trend) are needed to manage the pressure transient in the primary system (compare Figs. 6d with 5f). Both these effects are caused by the reduction of primary flow in the BZ circuit due to the PIE. The lower primary flow produces a decrease of the overall heat transfer coefficient in the BZ OTSGs, i.e., of the thermal power transferred to the secondary side. This increments the power load that must be managed by the primary pressure control system and, correspondingly, diminishes the one deputized to PCS SRVs.

Regarding the FW PHTS, the current accidental scenario is of no particular concern. Off-site power ensures the operation of primary pumps. After plasma termination, the lack of a source term, together with the presence of rated primary flow, leads water temperatures to converge to a common value, as reported in Fig. 6f. Sector 1 is used as reference. HITEC secondary flow is available at the transient beginning (see Section 4.1), guaranteeing enough cooling capability to remove the thermal power related to the plasma shutdown. For FW system, the

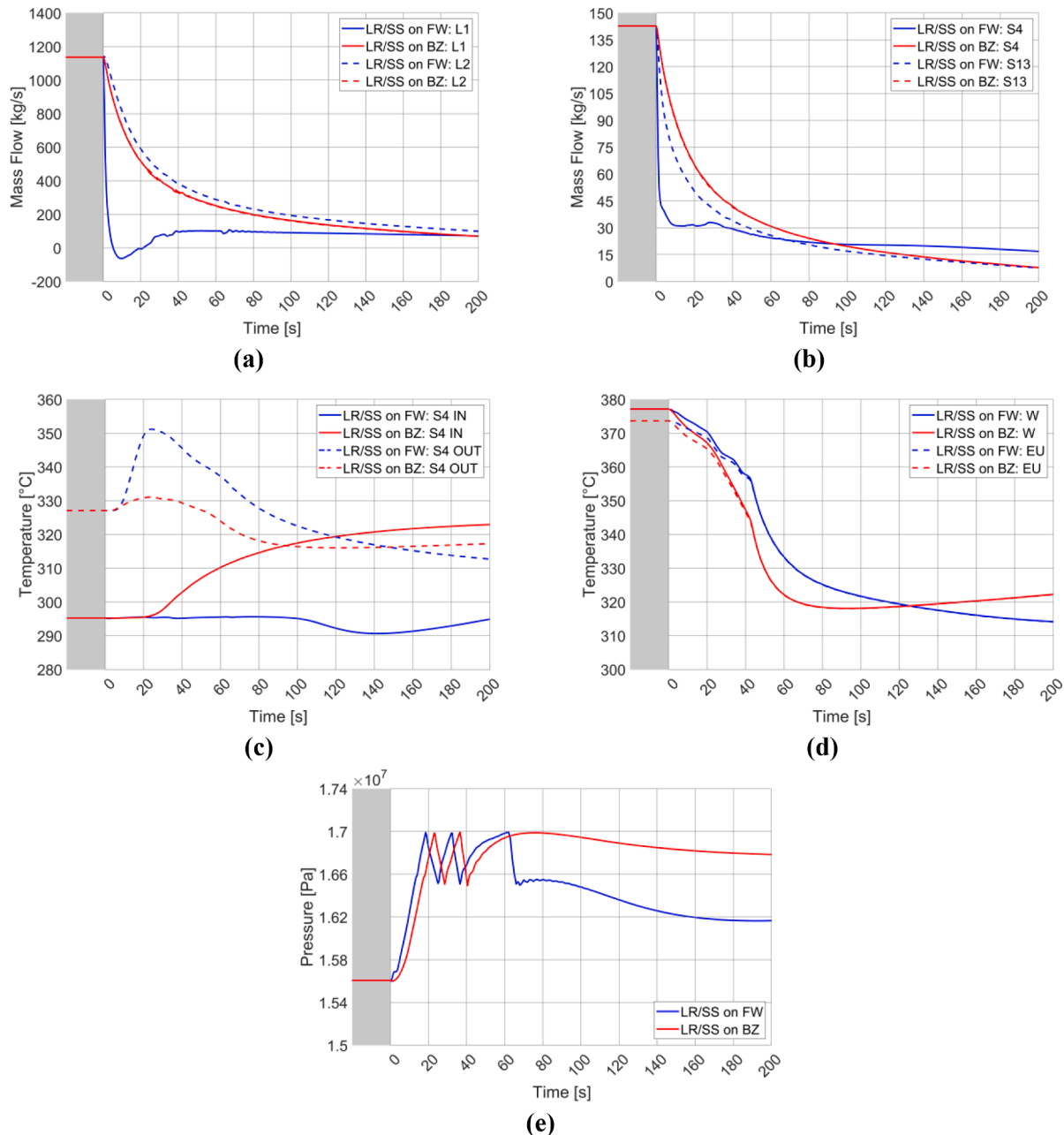


Fig. 7. Influence of LOSP on LR/SS accident, focus on FW PHTS: primary pumps mass flow (a); sectors 4 and 13 mass flow (b); water temperatures at BB inlet/outlet, sector 4 (c); Tungsten (W) and EUROFER (EU) temperatures related to FW component in sector 4 COB segment (d); system pressure (e).

pressure transient is similar to the one of the previous case (red line in Fig. 5f).

4.4. Influence of loss of off-site power

As stated in Sections 4.2 and 4.3, when LR/SS occurs, either involving a FW or a BZ pump, plasma termination and turbine trip are always triggered in less than one second from the PIE occurrence. In fact, flow associated with failed component rapidly drops and it is immediately detected by the control system. If LOSP is assumed to occur in combination with the initiating event, steam turbine is the only lasting component that can provide the AC power needed for primary pumps operation. This means that, when turbine trip is called, all BZ and FW PHTS MCPs (except the one affected by the initiating event) are cut off and start decelerating according to the torque/inertia equation. In

conclusion, when LR/SS and LOSP are considered together, in less than one second, even if for different reasons, all the primary pumps are off. This is visible in Fig. 7a and Fig. 8a, respectively referred to FW and BZ primary pumps. Whether or not PIE is located in a specific circuit (FW or BZ) mainly affects the flow symmetry in the related system (see blue lines in Fig. 7a and red lines in Fig. 8a). Such dissymmetry results in an uneven flow distribution between tokamak sectors (see Figs. 7b and 8b), with a more severe temperature transient for the ones nearest to the failed component (Figs. 7c and 8c). Also in this case, only parameters referred to sector 4 (worst case) and sector 13 (best case) are plotted. The behavior of the other sectors is enveloped. Dissymmetrical effects are more pronounced at the transient beginning due to the different decreasing trend associated with crashed component (sharp drop to zero in one second) with respect to the other system pumps (exponential trend due to torque/inertia equation). Also, their stopping times are

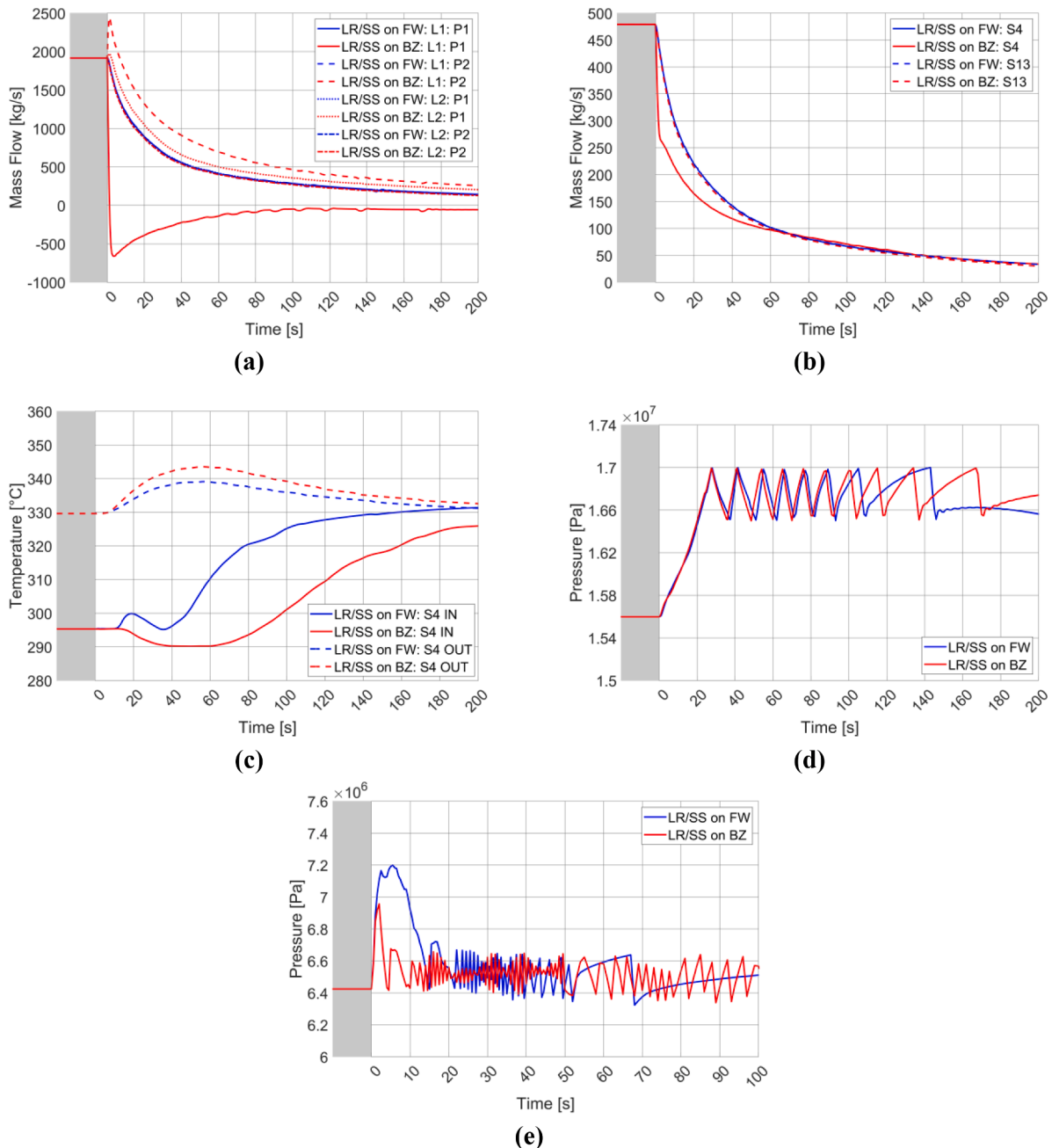


Fig. 8. Influence of LOSP on LR/SS accident, focus on BZ PHTS: primary pumps mass flow (a); sectors 4 and 13 mass flow (b); water temperatures at BB inlet/outlet, sector 4 (c); system pressure (d); PCS pressure (e).

different, but the influence of this parameter is negligible since less than one second occurs between PIE and turbine trip. In the long term, after all system pumps have stopped and natural circulation has established in both BZ and FW PHTSs, flow in the two loops and sixteen sectors returns quite symmetrical. Only a small deviation can be detected, mainly influencing the loop flows, caused by the broken pump acting as minor head loss due to the locked rotor or shaft seizure. Although, it is quite negligible. This aspect of BB PHTS long term behavior is well evidenced in [11].

In the early time after the PIE occurrence, because of the combination of the initiating event and the LOSP, both PHTSs lose nearly simultaneously: the power source (plasma termination is triggered), the heat sink (PCS Feedwater and IHTS flow are ramp-down) and the primary flow (primary pumps are crashed or stopped). The water temperatures at blanket inlet and outlet reported in Figs. 7c and 8c (respectively for FW and BZ sector 4, worst case) result from the relative balance between these decreasing parameters. Initially, the plasma power is prevalent, producing a temperature peak at BB outlet. The effect of the LOSP assumption on the maximum water temperature is clear. The loss of forced circulation in the primary cooling circuits causes the rise of this parameter. This can be detected in both PHTSs and in both accidental scenarios, i.e., LR/SS involving either BZ or FW system. The presence of PIE in a specific circuit furtherly increases water temperatures in the corresponding system, due to the sharp flow reduction caused by the failed pump. For BZ PHTS, the water temperature at sector 4 outlet reaches a maximum of 339 °C (50 s after the PIE occurrence) in case of broken component belonging to FW system, and of 344 °C (55 s after the PIE occurrence) if the failed pump is in BZ circuit. Such temperatures are below the saturation temperature referred to PHTS nominal pressure. Hence, no thermal crisis is expected in the DWTs. Regarding FW system, the maximum water temperature at sector 4 outlet is equals to 331 °C and 351 °C (both nearly at 20 s after the PIE occurrence), respectively for LR/SS involving BZ or FW system. In this latter case, the steam quality in the final section of the FW channels reaches nearly the 10%. The trend is similar to the one reported in Fig. 5d. LOSP assumption does not significantly affect this parameter (i.e. the dynamic of the transient in the first seconds after the PIE occurrence). Moreover, also in this scenario, the DNBR computed by RELAP5 is always $\gg 1$ and thus thermal crisis is expected to not occur in the cooling channels. The considerations made on this parameter in Section 4.2 are still valid. After the spike, system temperatures converge to a common value (see Figs. 7c and 8c) since the primary pump coast-down lasts longer than the plasma shutdown.

The initial power surplus is managed by the primary and secondary pressure control systems, as reported in Fig. 7e, Fig. 8d and Fig. 8e, respectively related to FW PHTS, BZ PHTS and PCS pressures. As discussed in Section 4.3, the loss of primary forced circulation strongly reduces the overall heat transfer coefficient within BZ OTSGs and FW HEXs (i.e., thermal exchange with the secondary side). As a consequence, the majority of the thermal power in excess must be dissipated by the PHTS PORVs, increasing the number of times the valve opens and closes (compare Fig. 7e with Fig. 5f and Fig. 8d with Fig. 6d). It is important to underline that the stop of all the system pumps also disables the pressurizer sprays. Hence, in these accidental transients, the PHTS PORVs become the first line of intervention against the over-pressurization.

Finally, for what concerns material temperatures (W and EU) related to FW component, they are reported in Fig. 7d. What is worth to be emphasized is that FW thermal inertia absorbs the water temperature spike also in these cases. The prevalent effect is still the plasma shutdown causing the decreasing temperature trends shown in the figure.

5. Conclusion

The main goal of the current simulation activity was to analyze the thermal-hydraulic performances of the DEMO WCLL blanket component

and related PHTS circuits during accidental conditions. To reach this objective, a complete model of the system was prepared by using RELAP5/Mod3.3 code. A modified version developed at DIAEE was used. It includes some new features, such as HITEC® thermal properties and heat transfer coefficient correlations, enhancing the code modeling capabilities with respect to fusion reactors. The thermal-hydraulic model was initially used to fully characterize the BB PHTS behavior during full plasma power state of DEMO normal operations. Control systems were implemented in the input deck to obtain all the design parameters and respect the DEMO requirements for this operative condition. This state was then used as initial condition to perform a transient analysis involving accidents belonging to the “Decrease in Coolant System Flow Rate” category. Locked Rotor/Shaft Seizure was selected as the PIE and investigated when involving either a BZ or a FW pump. Moreover, the influence on the accidental evolution of the Loss of Off-Site Power was also studied. In these simulations, control systems were disabled and a preliminary management strategy, based on the consolidated PWR experience, was proposed and implemented for some reactor components. In each case considered, the main blanket and PHTS parameters were assessed, such as mass flows, temperatures and pressures. The simulation outcomes proved the appropriateness of the current blanket and PHTS design in withstanding such accidental conditions. In all the transients analyzed, the occurrence of thermal crisis was not detected in both FW channels and DWTs. However, since no poloidal discretization was performed in the model developed for the current simulation activity, more detailed analyses in this field are recommended in the future development of the design activities. Finally, the implemented primary and secondary pressure control functions demonstrated to be able to manage the transients of this parameter in the corresponding systems in an effective way.

CRedit authorship contribution statement

C. Ciurluini: Conceptualization, Software, Formal analysis, Methodology, Writing – original draft, Writing – review & editing, Visualization. **M. D’Onorio:** Conceptualization, Methodology, Writing – original draft, Writing – review & editing. **F. Giannetti:** Conceptualization, Formal analysis, Methodology, Supervision, Writing – review & editing. **G. Caruso:** Conceptualization, Supervision, Writing – review & editing. **A. Del Nevo:** Conceptualization, Supervision.

Declaration of Competing Interest

The authors declare that they have no known competing financial interests or personal relationships that could have appeared to influence the work reported in this paper.

Data availability

No data was used for the research described in the article.

Acknowledgments

This work has been carried out within the framework of the EUROfusion Consortium, funded by the European Union via the Euratom Research and Training program (Grant Agreement No. 101052200 — EUROfusion). Views and opinions expressed are however those of the author(s) only and do not necessarily reflect those of the European Union or the European Commission. Neither the European Union nor the European Commission can be held responsible for them.

References

- [1] A.J.H. Donné, et al., European roadmap to fusion energy, in: *Proceedings of the Presentation at 2018 Symposium On Fusion Technology (SOFT)*, Giardini Naxos, Italy, 2018. September 16-21.
- [2] A. Del Nevo, et al., Recent progress in developing a feasible and integrated conceptual design of the WCLL BB in EUROfusion project, *Fusion Eng. Des.* 146 (2019) 1805–1809, <https://doi.org/10.1016/j.fusengdes.2019.03.040>.
- [3] G. Federici, et al., An overview of the EU Breeding Blanket design strategy as an integral part of the DEMO design effort, *Fusion Eng. Des.* 141 (2019) 30–42, <https://doi.org/10.1016/j.fusengdes.2019.01.141>.
- [4] E. Martelli, et al., Study of EU DEMO WCLL Breeding Blanket and primary heat transfer system integration, *Fusion Eng. Des.* 136 (2018) 828–833, <https://doi.org/10.1016/j.fusengdes.2018.04.016>.
- [5] L. Barucca, et al., Pre-conceptual design of EU DEMO balance of plant systems: objectives and challenges, *Fusion Eng. Des.* 169 (2021), 112504, <https://doi.org/10.1016/j.fusengdes.2021.112504>.
- [6] M. D'Onorio, et al., Preliminary safety analysis of an in-vessel LOCA for the EU-DEMO WCLL blanket concept, *Fusion Eng. Des.* 155 (2020), 111560, <https://doi.org/10.1016/j.fusengdes.2020.111560>.
- [7] M. D'Onorio, et al., Preliminary sensitivity analysis for an ex-vessel LOCA without plasma shutdown for the EU DEMO WCLL blanket concept, *Fusion Eng. Des.* 158 (2020), 111745, <https://doi.org/10.1016/j.fusengdes.2020.111745>.
- [8] X.Z. Jin, et al., LOFA analysis for the FW of DEMO HCPB blanket concept, in: *Proceedings of the 1st IAEA Technical Meeting on the Safety, Design and Technology of Fusion Power Plants*, Austria, Vienna, 2016, 3–5 May.
- [9] X.Z. Jin, BB LOCA analysis for the reference design of the EU DEMO HCPB blanket concept, *Fusion Eng. Des.* 136 (2018) 958–963, <https://doi.org/10.1016/j.fusengdes.2018.04.046>.
- [10] C. Ciurluini, et al., Analysis of the thermal-hydraulic behavior of the EU-DEMO WCLL Breeding Blanket cooling systems during a loss of flow accident, *Fusion Eng. Des.* 164 (2021), 112206, <https://doi.org/10.1016/j.fusengdes.2020.112206>.
- [11] C. Ciurluini, et al., Study of the EU-DEMO WCLL Breeding Blanket primary cooling circuits thermal-hydraulic performances during transients belonging to LOFA category, *Energies* 14 (6) (2021) 1541, <https://doi.org/10.3390/en14061541>.
- [12] *The US Nuclear Regulatory Commission (USNRC), RELAP5/MOD3 Code Manual: Code Structure, System Models, and Solution Methods, Volume I*, USNRC, Washington, DC, USA, 1998. NUREG/CR-5535.
- [13] F. Edemetti, et al., Optimization of the first wall cooling system for the DEMO WCLL blanket, *Fusion Eng. Des.* 161 (2020), 111903, <https://doi.org/10.1016/j.fusengdes.2020.111903>.
- [14] F. Edemetti, et al., Thermal-hydraulic analysis of the DEMO WCLL elementary cell: BZ tubes layout optimization, *Fusion Eng. Des.* 160 (2020), 111956, <https://doi.org/10.1016/j.fusengdes.2020.111956>.
- [15] Coastal Chemical Co. L.L.C., "HITEC® Heat Transfer Salt technical brochure." Available online: <https://coastalchem.com/products/heat-transfer-fluids/hitec-heat-transfer-salt>. Visited on 1st September 2022.
- [16] E.N. Sieder, G.E. Tate, Heat transfer and pressure drop of liquids in tubes, *J. Ind. Eng. Chem.* 28 (1936) 1429–1435, <https://doi.org/10.1021/ie50324a027>.
- [17] I.E. Idelchik, *Handbook of Hydraulic Resistance*, 2nd ed., Hemisphere Publishing Corporation, Washington DC, USA, 1986.
- [18] A. Spagnuolo, et al., Development of load specifications for the design of the Breeding Blanket system, *Fusion Eng. Des.* 157 (2020), 111657, <https://doi.org/10.1016/j.fusengdes.2020.111657>.